biology and life sciences forum

Proceeding Paper

Water-Sorption Isotherms and Air-Drying-Kinetics Modelling of Andean Tubers and Tuberous Roots

Liliana Acurio, Ariel Baquerizo, Alexandra Borja, Marcelo Vayas, Purificación García-Segovia, Javier Martínez-Monzó and Marta Igual

MDPI

https://doi.org/10.3390/Foods2023-15141

biology and life sciences forum

MDPI

Proceeding Paper

Water-Sorption Isotherms and Air-Drying-Kinetics Modelling of Andean Tubers and Tuberous Roots †

Liliana Acurio [1,2,*], Ariel Baquerizo [1], Alexandra Borja [1], Marcelo Vayas [1], Purificación García-Segovia [2], Javier Martínez-Monzó [2] and Marta Igual [2,*]

[1] Food and Biotechnology Science and Engineering Department, Technical University of Ambato, Av. Los Chasquis & Río Payamino, Ambato 180150, Ecuador

[2] i-Food Group, Instituto Universitario de Ingeniería de Alimentos-FoodUPV, Universitat Politècnica de València, Camino de Vera s/n, 46021 Valencia, Spain; xmartine@tal.upv.es (J.M.-M.)

* Correspondence: lp.acurio@uta.edu.ec (L.A.); marigra@upvnet.upv.es (M.I.); Tel.: +593-986090742 (L.A.); +34-625430677 (M.I.)

† Presented at the 4th International Electronic Conference on Foods, 15–30 October 2023; Available online: https://foods2023.sciforum.net/.

Abstract: In recent years, scientific research has focused on studying Andean roots and tubers due to their attractive agricultural and nutritional qualities; however, as they contain a high level of moisture, it is imperative to dry them to extend their useful life. Likewise, analysing food-drying kinetics and food stability (regarding water activity) is essential to control moisture removal and the marketing progress. The drying process carried out in this study (65 °C for 8 h) showed three clear stages: adaptation, the drying period at a constant velocity, and a third stage with a gradual drop in the drying rate. The experimental data were satisfactorily adjusted to seven mathematical models, with the Page model highlighted since it presented higher coefficient-of-determination values. Likewise, this model estimated that the mean-error and percentage-of-relative-mean-deviation values were less than 1. The isotherms showed a type-II sigmoidal shape, showing that the samples were hygroscopic due to the structural changes undergone by the matrix during the process. Finally, the GAB model showed a higher coefficient of determination. All the Andean tubers and tuberous root flours must be dried until reaching a humidity below 10 $g_{water}/g_{dry\ mass}$ and stored in environments with a relative humidity lower than 60% to remain stable for longer.

Keywords: ipomoea batatas; tropaeolum tuberosum; arracacia xanthorrhiza; oxalis tuberosa

Citation: Acurio, L.; Baquerizo, A.; Borja, A.; Vayas, M.; García-Segovia, P.; Martínez-Monzó, J.; Igual, M. Water-Sorption Isotherms and Air-Drying-Kinetics Modelling of Andean Tubers and Tuberous Roots. *Biol. Life Sci. Forum* **2023**, *26*, 71. https://doi.org/10.3390/Foods2023-15141

Academic Editor: Jean-Christophe Jacquier

Published: 17 October 2023

1. Introduction

In recent years, scientific research has focused on studying underutilized autochthonous crops worldwide. Among these crops are the roots produced in the Andes mountain range. Numerous scientific articles report their peculiar cultivation properties, such as their high adaptability to temperature fluctuations and resistance to pests [1]. There is also scientific evidence of the excellent nutritional qualities of these roots. For example, sweet potato (*Ipomoea batatas* (L.) Lam.) shows high values of protein, fibers, vitamin B, iron, calcium, and bioactive compounds [2]. Mashua (*Tropaeolum tuberosum* Ruiz and Pavón) contains many glucosinolates, polyphenols, isothiocyanates, and anthocyanins that act against plagues and diseases. Also, this root is an excellent provider of vitamin C and provitamin A [3]. Zanahoria blanca (*Arracacia xanthorrhiza* Bancr.) has important values for thiamine, niacin, vitamin A, and ascorbic acid [4]. Finally, oca (*Oxalis tuberosa* Molina) presents a high starch quantity (60% of the dry weight) [5], and it is a useful provider of protein, fructooligosaccharides, iron, and riboflavin [6].

Convection hot air drying is used mainly in industries to produce dried fruits and vegetables, even though it is not energy efficient and requires more time to reach a low level of moisture. The drying kinetics are essential to controlling the moisture removal progress and drying variables (the drying rate, moisture diffusivity, and activation energy) [7]. An advantage is that this experiment can be conducted on a laboratory scale. Likewise, modelling the drying kinetics is necessary to optimize the process and propose improvements to the drier before it is built on a pilot scale. Food stability is essential in packaging, and a_w is directly related to chemical and microbial changes. Some studies have demonstrated that an a_w increase beyond 0.4 will induce a 50–100% increase in the degradation rate [8]. In this sense, the water-sorption isotherms can predict the product's shelf life by modelling the possible moisture changes during storage.

The aims of the present work are (1) to determine the modelling of the corresponding drying kinetics and (2) to determine the water-sorption-isotherm modelling of sweet potato, mashua, zanahoria blanca, and three varieties of oca (white, yellow, and red).

2. Materials and Methods

2.1. Raw Materials and Sample Preparation

Sweet potato (*I. batatas* (L.) Lam.), mashua (*T. tuberosum* Ruiz & Pavón), zanahoria blanca (*Arracacia xanthorrhiza* Bancr.), and three varieties of Oca (*O. tuberosa* Molina) (white, yellow, and red) were purchased from a local market in Ambato, Ecuador. The roots were peeled and cut into slices (2 mm). Slices were pretreated in microwaves (750 W/20 s) and then submerged in water at 4 °C/20 s [9]. This pretreatment was considered necessary because preliminary tests showed that these roots tend to brown due to enzymes and generate undesirable colors. The microwave energy ranges between 1.24×10^{-6} and 1.24×10^{-3} eV, and some studies have demonstrated that it does not affect molecular structure since it is lower than the ionization energies of biological compounds (13.6 eV), bond energies (2–5 eV), and van der Waals interactions (<2 eV) [10,11]. Also, Shen et al. [12] demonstrated a decrease in the double-helix structure of potato starch after microwaving at 1000 W, and Lewandowicz et al. [13] showed crystallinity pattern changes after microwaving at 800 W. For this reason, pretreatment was carried out at a lower energy (750 W).

2.2. Determination of Drying Kinetics

Fresh-peeled slices (2 mm) were used to determine the initial water content (x_w). This determination was carried out in a Vaciotem vacuum oven (J.P. Selecta, Barcelona, Spain) set to 103 °C for 48 h. The slices were dried via convection in an air drier (model CD 160, Gander Mountain, Saint Paul, MN, USA) at 65 °C for 8 h, with the air velocity (2 m s^{-1}) kept constant [14]. The drying temperature was established based on preliminary tests and the results obtained in a study on similar roots grown in the same area (lower temperature for a long time/60 °C for 24 h) [15].

Samples were placed on a metallic mesh (450 × 450 mm), allowing a transversal airflow. Drying kinetics were determined via weighing in a precision analytical balance (Mettler Toledo, Greifensee, Switzerland). The weight was measured every 10 min during the first 2 h and, subsequently, every 30 min until the drying time was complete (8 h). These experiments were performed on 9 slices of each sample. The water content (x_w) was obtained through vacuum drying the pieces in a vacuum oven (Vaciotem, J.P. Selecta, Barcelona, Spain) at 103 °C for 48 h.

Drying Kinetics: Mathematical Modelling

Experimental data of drying kinetics were fitted to the models shown in Table 1.

Table 1. Equations used for modelling the drying kinetics.

Model	Equation	Equation Number	References
Newton	$MR = Exp(-kt)$	(1)	[16]
Page	$MR = Exp(-kt^n)$	(2)	[17]
Modified Page	$MR = Exp(-kt)^n$	(3)	[18]
Henderson and Pabis	$MR = a \times Exp(-kt)$	(4)	[19]
Logarithmic	$MR = a \times Exp(-kt) + c$	(5)	[20]
Thomson	$MR = 1 + at + bt^2$	(6)	[21]
Fick	$MR = \frac{X-X_e}{X_o-X_e} = \frac{8}{\pi^2}\Sigma_{n=1}^{\infty}\frac{1}{(2n-1)^2}\exp(-(2n-1)^2\frac{\pi^2 D_{eff}}{4\times L^2}\times t)$	(7)	[22]

where MR represents the amount of moisture remaining in the samples reported to the initial moisture content; t is the time (h); n is the drying exponent; and a, b, c, and k are the drying constants.

2.3. Determination of Water-Sorption Isotherms

The gravimetric method used saturated salt solutions to determine the equilibrium moisture content (Table 2) [23]. The saline solutions used were of reagent grade, and the preparation method was adopted from W Spiess and Wolf [24]. To inhibit microbial growth, thymol was added in $a_w \geq 0.5$. Water sorption experiments were carried out at 20 °C (±1 °C). The sorption isotherm is of particular importance in the determination of a drying endpoint, microbiological safety, and the prediction of shelf life; for this reason, the authors chose to experiment with the average annual temperature (20 ± 1 °C) [25] reported in the Andean area interested in the development of the technology, and where the flour obtained will be marketed (Ambato, Ecuador).

Table 2. Saturated salt solutions are used in the determination of water-sorption isotherms.

Name	Nomenclature	a_w *	Name	Nomenclature	a_w *
Lithium chloride	$LiCl$	0.1178	Sodium bromide	$NaBr$	0.5732
Potassium acetate	CH_3CO_2K	0.2982	Ammonium sulphate	$(NH_4)_2SO_4$	0.8012
Magnesium chloride	$MgCl_2$	0.3425			

* Values were determined using the AquaLab 4TE water activity meter (Decagon Devices, Inc., Pullman, WA, USA).

Samples were weighed in a precision analytical balance (Mettler Toledo, Greifensee, Switzerland) at regular intervals until reaching constant weight (±0.0005 g), the moment at which it is considered that the moisture content of samples achieved the equilibrium (12 weeks).

Water-Sorption Isotherms: Mathematical Modelling

Experimental data were fitted to the models shown in Table 3.

Table 3. Equations used for modelling the sorption isotherms.

Model	Equation	Equation Number	References
Brunauer, Emmett, and Teller (BET)	$X_e = \frac{X_0\times C\times a_w}{(1-a_w)\times(1+(C-1)\times a_w)}$	(8)	[26]
Guggenheim, Anderson, and de Boer (GAB)	$X_e = \frac{X_0\times C\times K\times a_w}{(1-(K\times a_w))\times(1+(C-1)\times(K\times a_w))}$	(9)	[27]

where X_e is the equilibrium moisture content ($g_{water}/g_{dry\ mass}$); X_0 is the monolayer moisture content ($g_{water}/g_{dry\ mass}$); C is the empirical constant (dimensionless) for the BET and GAB equations; and K is the second empirical constant (dimensionless) for the GAB equation.

2.4. Statistical Analysis

The goodness of the fit was evaluated based on the coefficient of determination (r^2), root-mean-square error (RMSE), and mean relative percentage deviation (MRPD).

Statgraphics Centurion XVII Software, version 17.2.04 (Statgraphics Technologies, Inc., The Plains, VA, USA) was used in the analyses.

3. Results and Discussion

3.1. Drying Kinetics

Figure 1a shows the experimental drying kinetic curves. A sudden decrease in humidity is evident in the first 4 h of drying. A trend change is observed, since the food has transferred the most significant amount of free water. Figure 1b represents the drying-rate curve. An adaptation period is observed in all samples in the first 30 min, in which the interface temperature increased to reach the drying conditions. Subsequently, the constant velocity period was marked for 30 min. In this phase, the samples lose moisture at $1054 \pm 249\ g_{water}/h \times m^2$ until reaching the critical humidity. This phase depends directly on the product, temperature, relative humidity of the air, flow direction, and food thickness [28]. The third stage showed a gradual drop in the drying rate, because the superficial layer of water in the food had evaporated entirely. In this period, the drying rate completely decays ($18 \pm 9\ g_{water}/h \times m^2$).

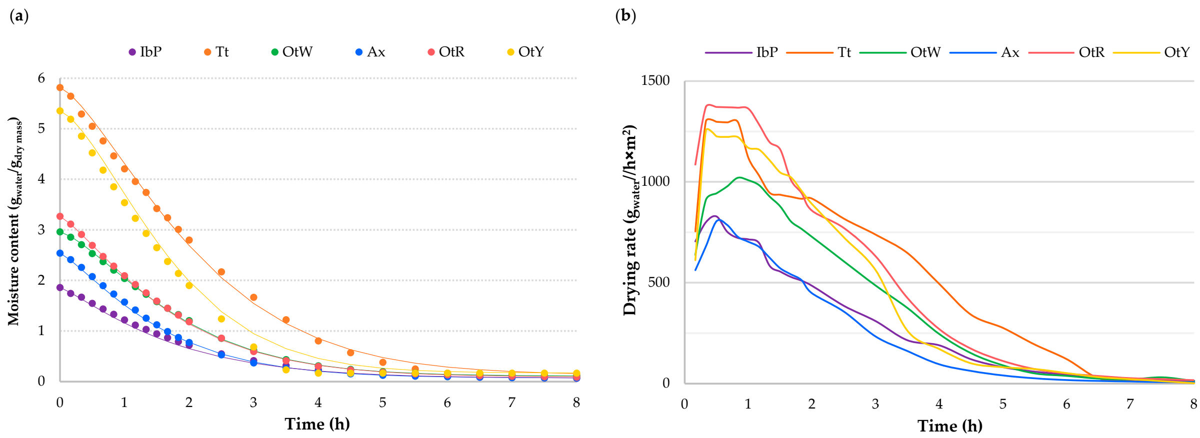

Figure 1. (**a**) Experimental and estimated drying kinetic curves using the Page model, (**b**) drying rates versus free moisture content ($g_{water}/g_{dry\ mass}$) (IbP: purple sweet potato, Tt: mashua, Ax: zanahoria blanca, OtW: oca white variety, OtY: oca yellow variety, OtR: oca red variety).

Drying Kinetics: Mathematical Modelling

The coefficient-of-determination values (r^2) were higher in the Page model (Table 4). Likewise, the RMSE and MRPD were less than 1 in this model. The parameter *k* represents the movement of moisture inside the food and the transfer to the surface of the air; therefore, higher values represent a faster drying process [29]. The Fick model yielded effective diffusivity values from 2.22 to 2.92 $\times 10^{-7}$ m^2/s; this value in food oscillates between 1×10^{-6} and 1×10^{-11} m^2/s [30]. The variation in the diffusivity depends on the drying conditions (the temperature, pressure, and velocity) and the matrix (its structure, size, and composition) [31].

Table 4. Parameters obtained in the drying-kinetics mathematical modelling.

Sample		Models						
		Newton	Page	Modified Page	Henderson and Pabis	Logarithmic	Thomson	Fick
IbP (Sweet potato)	Model constants	*k*: 0.691	*k*: 0.4985 *n*: 1.173	*k*: 0.5524 *n*: 1.173	*k*: 0.704 *a*: 1.4597	*k*: 0.518 *a*: 1.082 *c*: 0.0394	*a*: 0.3497 *b*: 0.0298	*Def:* 2.619×10^{-7}
	Adj. r^2	0.982	0.9923	0.9923	0.988	0.9586	0.99	0.9611
	RMSE	0.134	0.027	4.051	5.0432	0.9293	0.1169	2.232
	MRPD	0.528	0.0265	11.9376	18.6275	4.2325	3.94	10.877

Table 4. *Cont.*

Sample		Models						
		Newton	Page	Modified Page	Henderson and Pabis	Logarithmic	Thomson	Fick
Tt (Mashua)	Model constants	*k*: 0.66	*k*: 0.308 *n*: 1.375	*k*: 0.4245 *n*: 1.375	*k*: 0.738 *a*: 2.059	*k*: 0.3136 *a*: 1.192 *c*: 0.1465	*a*: 0.2788 *b*: 0.0185	*Def*: 2.4953×10^{-7}
	Adj. r^2	0.8962	0.989	0.989	0.9244	0.9363	0.9977	0.8627
	RMSE	1.014	0.196	5.582	23.8585	3.5523	23.8585	4.1564
	MRPD	1.086	0.1234	0.1184	22.1583	4.0482	22.1583	5.574
Ax (Zanahoria blanca)	Model constants	*k*: 0.7684	*k*: 0.5399 *n*: 1.2194	*k*: 0.6164 *n*: 1.2194	*k*: 0.75 *a*: 1.3872	*k*: 0.6151 *a*: 1.08 *c*: 0.0262	*a*: 0.3746 *b*: 0.0337	*Def*: 2.9196×10^{-7}
	Adj. r^2	0.995	0.9977	0.999	0.9864	0.9636	0.9636	0.996
	RMSE	0.171	0.039	4.4474	6.4694	1.1864	1.1864	2.632
	MRPD	0.521	0.121	9.8944	18.841	4.1582	4.1582	10.49
OtW (Oca white variety)	Model constants	*k*: 0.7261	*k*: 0.3893 *n*: 1.3656	*k*: 0.2037 *n*: 1.3656	*k*: 0.745 *a*: 1.6428	*k*: 0.4682 *a*: 1.14 *c*: 0.0645	*a*: 0.3569 *b*: 0.0296	*Def*: 2.762×10^{-7}
	Adj. r^2	0.9845	0.9986	0.999	0.9497	0.952	0.9955	0.9887
	RMSE	1.2457	0.023	4.755	8.122	1.3943	0.16	2.6244
	MRPD	0.9342	0.013	7.5582	19.32	4.11	3.95	8.8533
OtY (Oca yellow variety)	Model constants	*k*: 0.8689	*k*: 0.3816 *n*: 1.46	*k*: 1.5997 *n*: 1.291	*k*: 0.922 *a*: 2.139	*k*: 0.444 *a*: 1.158 *c*: 0.082	*a*: 0.3523 *b*: 0.0285	*Def*: 2.7851×10^{-7}
	Adj. r^2	0.9727	0.9921	0.976	0.888	0.9464	0.9953	0.9727
	RMSE	3.129	20.376	5.216	23.1519	1.286	11.6696	4.0237
	MRPD	1.2	18.901	2.684	30.15	0.422	16.451	5.7033
OtR (Oca red variety)	Model constants	*k*: 0.7743	*k*: 0.4692 *n*: 1.243	*k*: 1.838 *n*: 1.243	*k*: 0.7 *a*: 1.4396	*k*: 0.527 *a*: 1.089 *c*: 0.038	*a*: 0.3525 *b*: 0.03	*Def*: 2.2283×10^{-7}
	Adj. r^2	0.991	0.998	0.9997	0.9822	0.9685	0.9893	0.9905
	RMSE	0.127	7.4486	4.765	3.78	0.5553	3.151	1.9936
	MRPD	0.226	17.252	11.927	12.376	0.4327	10.973	6.5661

3.2. Water-Sorption Isotherms

The samples showed type-II isotherms (Figure 2), also called sigmoidal, since they present an inflection point. Similar results have been reported in cassava flour [32]. The isotherm curve showed that the matrix is highly hygroscopic, since the higher the environment's relative humidity, the greater the flour's capacity for the water molecules' adsorption. This shows that the drying and grinding process causes structural changes in the food matrix that influence an increase in the active points of water adsorption [33].

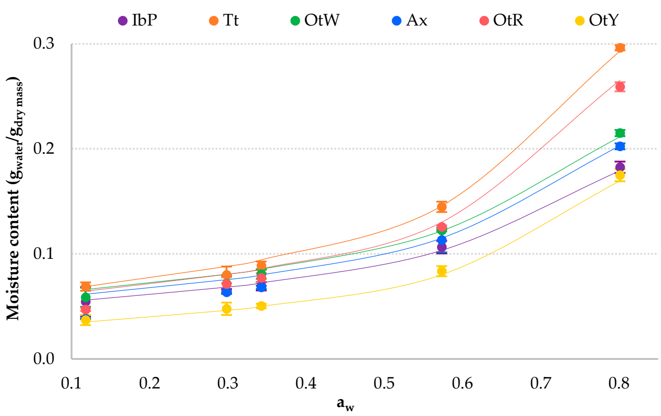

Figure 2. Experimental water-sorption isotherms at 20 °C and estimated curves using the GAB model (IbP: purple sweet potato, Tt: mashua, Ax: zanahoria blanca, OtW: oca white variety, OtY: oca yellow variety, OtR: oca red variety).

Water-Sorption Isotherms. Mathematical Modelling

The BET model was correctly adjusted up to an a_w of 0.57, while the GAB model was adjusted in the entire evaluated range; likewise, the GAB model presented a higher r^2. Similar results were observed in sweet potato flour (*Ipomoea batata* L.) [34]. The parameters are reported in Table 5.

Table 5. Parameters obtained in the water-sorption isotherm mathematical modelling.

Samples		Models		Samples		Models		Samples		Models	
		BET	GAB			BET	GAB			BET	GAB
Sweet potato	Model constants	X_0: 0.04 *C*: 17.875	X_0: 0.05 *C*: 17.79 *K*: 0.9	Oca white variety	Model constants	X_0: 0.05 *C*: 12.5	X_0: 0.059 *C*: 13.82 *K*: 0.9	Oca yellow variety	Model constants	X_0: 0.051 *C*: 4.443	X_0: 0.053 *C*: 4.795 *K*: 0.97
	Adj. r^2	0.98	0.999		Adj. r^2	0.98	0.98		Adj. r^2	0.98	0.97
	RMSE	0.016	0.022		RMSE	0.0032	0.0037		RMSE	0.02	0.023
	MRPD	19.98	19.99		MRPD	7.052	7.154		MRPD	12.72	13.74
Mashua	Model constants	X_0: 0.065 *C*: 16.4	X_0: 0.07 *C*: 11.47 *K*: 0.96	Zanahoria blanca	Model constants	X_0: 0.051 *C*: 15.24	X_0: 0.055 *C*: 12.13 *K*: 0.91	Oca red variety	Model constants	X_0: 0.055 *C*: 21.89	X_0: 0.057 *C*: 20.26 *K*: 0.98
	Adj. r^2	0.989	0.999		Adj. r^2	0.972	0.988		Adj. r^2	0.989	0.998
	RMSE	0.004	0.005		RMSE	0.01	0.013		RMSE	0.01	0.011
	MRPD	19.999	19.999		MRPD	19.07	19.87		MRPD	12.56	13.74

The moisture of the monolayer (X_0) determines the bound moisture of the food [35]. The constant *C* is known as the sorption heat and relates the active sites of the food matrix and the water molecules of the atmosphere. The shape curve is related to the *C* value; when its value is greater than 2, this means there is an inflection point in the curve. Therefore, the isotherm is type II, and the food shows an adsorption capacity of water in multilayers. The correction factor of the multilayer sorption constant (*K*) of the GAB model should be <1, and it represents the interaction of water molecules in the multilayer [36].

4. Conclusions

The drying process at 65 °C for 8 h showed three precise stages. The first stage of adaptation was where the humidity of the food was reduced minimally—subsequently, the drying period was at a constant velocity, presenting an approximately linear trend. The third stage showed a gradual drop in the drying rate. The experimental data were satisfactorily adjusted to seven mathematical models, highlighting the Page model (higher r^2). The isotherms showed a type-II sigmoidal shape, showing that the samples are hygroscopic due to the structural changes undergone during the process. All the matrices must be dried until they reach a humidity below 10 $g_{water}/g_{dry\ mass}$ and stored in environments with an HR lower than 60% to remain stable. Finally, the GAB showed a higher r^2.

Author Contributions: Conceptualization, L.A. and M.I.; data curation, L.A., A.B. (Ariel Baquerizo), A.B. (Alexandra Borja) and M.V.; writing—original draft preparation, L.A.; writing—review and editing, P.G.-S., J.M.-M. and M.I. All authors have read and agreed to the published version of the manuscript.

Funding: This research received no external funding.

Institutional Review Board Statement: Not applicable.

Informed Consent Statement: Not applicable.

Data Availability Statement: The data are contained within the article.

Acknowledgments: The authors are grateful to the Centro de Cooperación al Desarrollo (CCD) of the Universitat Politècnica de València (project AD2111) and the Dirección de Investigación y Desarrollo (DIDE) of the Technical University of Ambato (Resolution UTA-CONIN-2022-0269-R), for financing the project "Valorización de tubérculos andinos para la obtención de ingredientes alimentarios y su viabilidad. Concienciación de su valor nutritivo y funcional".

Conflicts of Interest: The authors declare no conflict of interest.

References

1. Flores, H.E.; Walker, T.S.; Guimarães, R.L.; Bais, H.P.; Vivanco, J.M. Andean root and tuber crops: Underground rainbows. *HortScience* **2003**, *38*, 161–168. [CrossRef]
2. Alam, M.K. A comprehensive review of sweet potato (*Ipomoea batatas* [L.] Lam): Revisiting the associated health benefits. *Trends Food Sci. Technol.* **2021**, *115*, 512–529. [CrossRef]
3. Guevara-Freire, D.A.; Valle-Velástegui, L.; Barros-Rodríguez, M.; Vásquez, C.; Zurita-Vásquez, H.; Dobronski-Arcos, J.; Pomboza-Tamaquiza, P. Nutritional composition and bioactive components of mashua (*Tropaeolum tuberosum* Ruiz and Pavón). *Trop. Subtrop. Agroecosyst.* **2018**, *21*, 53–68. [CrossRef]
4. Ayala, G. Aporte de los cultivos andinos a la nutrición humana. In *Raíces Andinas: Contribuciones al Conocimiento y a la Capacitación. I. Aspectos Generales y Recursos Genéticos de las Raíces Andinas*; Seminario, J., Ed.; International Potato Center: Lima, Peru, 2004; pp. 101–112.
5. Zhu, F.; Cui, R. Comparison of physicochemical properties of oca (*Oxalis tuberosa*), potato, and maize starches. *Int. J. Biol. Macromol.* **2020**, *148*, 601–607. [CrossRef] [PubMed]
6. Jimenez, M.E.; Rossi, A.; Sammán, N. Health properties of oca (*Oxalis tuberosa*) and yacon (*Smallanthus sonchifolius*). *Food Funct.* **2015**, *6*, 3266–3274. [CrossRef] [PubMed]
7. Aniesrani Delfiya, D.; Prashob, K.; Murali, S.; Alfiya, P.; Samuel, M.P.; Pandiselvam, R. Drying kinetics of food materials in infrared radiation drying: A review. *J. Food Process Eng.* **2022**, *45*, e13810. [CrossRef]
8. Troller, J. *Water Activity and Food*; Elsevier: Amsterdam, The Netherlands, 2012.
9. Wang, J.; Yang, X.-H.; Mujumdar, A.; Wang, D.; Zhao, J.-H.; Fang, X.-M.; Zhang, Q.; Xie, L.; Gao, Z.-J.; Xiao, H.-W. Effects of various blanching methods on weight loss, enzymes inactivation, phytochemical contents, antioxidant capacity, ultrastructure and drying kinetics of red bell pepper (*Capsicum annuum* L.). *LWT* **2017**, *77*, 337–347. [CrossRef]
10. Shazman, A.; Mizrahi, S.; Cogan, U.; Shimoni, E. Examining for possible non-thermal effects during heating in a microwave oven. *Food Chem.* **2007**, *103*, 444–453. [CrossRef]
11. Farhat, A.; Fabiano-Tixier, A.-S.; El Maataoui, M.; Maingonnat, J.-F.; Romdhane, M.; Chemat, F. Microwave steam diffusion for extraction of essential oil from orange peel: Kinetic data, extract's global yield and mechanism. *Food Chem.* **2011**, *125*, 255–261. [CrossRef]
12. Shen, H.; Fan, D.; Huang, L.; Gao, Y.; Lian, H.; Zhao, J.; Zhang, H. Effects of microwaves on molecular arrangements in potato starch. *RSC Adv.* **2017**, *7*, 14348–14353. [CrossRef]
13. Lewandowicz, G.; Fornal, J.; Walkowski, A. Effect of microwave radiation on physico-chemical properties and structure of potato and tapioca starches. *Carbohydr. Polym.* **1997**, *34*, 213–220. [CrossRef]
14. Acurio, L.; Salazar, D.; García-Segovia, P.; Martínez-Monzó, J.; Igual, M. Third-Generation Snacks Manufactured from Andean Tubers and Tuberous Root Flours: Microwave Expansion Kinetics and Characterization. *Foods* **2023**, *12*, 2168. [CrossRef]
15. Salazar, D.; Arancibia, M.; Ocaña, I.; Rodríguez-Maecker, R.; Bedón, M.; López-Caballero, M.E.; Montero, M.P. Characterization and technological potential of underutilized ancestral andean crop flours from Ecuador. *Agronomy* **2021**, *11*, 1693. [CrossRef]
16. O'Callaghan, J.R.; Menzies, D.J.; Bailey, P.H. Digital simulation of agricultural drier performance. *J. Agric. Eng. Res.* **1971**, *16*, 223–244. [CrossRef]
17. Page, G.E. *Factors Influencing the Maximum Rates of Air Drying Shelled Corn in Thin Layers*; Purdue University: West Lafayette, IN, USA, 1949.
18. Overhults, D.G.; White, G.; Hamilton, H.; Ross, I. Drying soybeans with heated air. *Trans. ASAE* **1973**, *16*, 112. [CrossRef]
19. Henderson, S.M.; Pabis, S. Grain drying theory, I. Temperature effect on drying coefficient. *J. Agric. Eng. Res.* **1961**, *6*, 169–173.
20. Yagcioglu, A. Drying characteristic of laurel leaves under different conditions. In Proceedings of the 7th International Congress on Agricultural Mechanization and Energy, Adana, Turkey, 26–27 May 1999; pp. 565–569.
21. Thompson, T.L.; Peart, M.; Foster, G.H. Mathematical Simulation of Corn Drying—A New Model. *Trans. ASAE* **1968**, *11*, 582–0586. [CrossRef]
22. Crank, J. *The Mathematics of Diffusion*; Oxford University Press: Oxford, UK, 1979.
23. Greenspan, L. Humidity fixed points of binary saturated aqueous solutions. *J. Res. Natl. Bur. Stand.* **1977**, *81*, 89. [CrossRef]
24. Spiess, W.E.; Wolf, W. Critical evaluation of methods to determine moisture sorption isotherms. In *Water Activity: Theory and Applications to Food*; Routledge: London, UK, 2017; pp. 215–233.
25. Honorable Provincial Government of Tungurahua. Tungurahua Hydrometeological Network. Available online: https://rrnn.tungurahua.gob.ec/red/promedios_mensuales (accessed on 14 October 2023).
26. Brunauer, S.; Emmett, P.H.; Teller, E. Adsorption of gases in multimolecular layers. *J. Am. Chem. Soc.* **1938**, *60*, 309–319. [CrossRef]
27. Van den Berg, C.; Bruin, S. Water activity and its estimation in food systems. In Proceedings of the International Symposium Properties of Water in Relation to Food Quality and Stability, Osaka, Japan, 10–16 September 1978.
28. Restrepo Victoria, Á.H.; Burbano Jaramillo, J.C. Disponibilidad térmica solar y su aplicación en el secado de granos. *Sci. et Tech.* **2005**, *1*, 127–132.
29. Ananias, R.A.; Vallejos, S.; Salinas, C. Estudio de la cinética del secado convencional y bajo vacío del pino radiata. *Maderas. Cienc. y Tecnol.* **2005**, *7*, 37–47. [CrossRef]

30. García-Mogollón, C.; Torregroza-Espinosa, A.; Sierra-Bautista, M. Cinética de Secado de Chips de Yuca (*Manihot esculenta* crantz) en Horno Microondas. *Rev. Técnica De la Fac. De Ing. Univ. del Zulia* **2016**, *39*, 098–103.
31. Salcedo-Mendoza, J.; Contreras-Lozano, K.; García-López, A.; Fernandez-Quintero, A. Modelado de la cinética de secado del afrecho de yuca (*Manihot esculenta* Crantz). *Rev. Mex. De Ing. Química* **2016**, *15*, 883–891. [CrossRef]
32. Navia, D.; Ayala, A.; Villada, H.S. Isotermas de adsorción de bioplásticos de harina de yuca moldeados por compresión. *Biotecnol. En El Sect. Agropecu. Y Agroindustrial* **2011**, *9*, 77–87.
33. Martins Oyinloye, T.; Byong Yoon, W. Effect of freeze-drying on quality and grinding process of food produce: A review. *Processes* **2020**, *8*, 354. [CrossRef]
34. Saavedra Layza, G.E. Effect of Temperature on the Monolayer Value of Sweet Potato (*Ipomoea batata* L.) Flour Yellow Variety through the GAB Isotherm. Bachelor's Thesis, National University of Trujillo, Trujillo, Perú, 2022.
35. Gutierrez Balarezo, J.; Diaz Viteri, J.E.; Mendieta Taboada, O.W.; Pulla Huilca, P.V.; Chañi Paucar, L.O. Conservación de la harina de plátano (*Musa paradisiaca*) en Puerto Maldonado, Madre de Dios. *Biodivers. Amaz.* **2019**, *4*, 74–86.
36. Ceballos, A.M.; Giraldo, G.I.; Orrego, C.E. Evaluacion de varios modelos de isotermas de adsorcion de agua de un polvo de fruta deshidratada. *Vector* **2009**, *1*, 107–117.